Chinese Journal of Physics 61 (2019) 155–165

Contents lists available at ScienceDirect

Chinese Journal of Physics

journal homepage: www.elsevier.com/locate/cjph

Ferromagnetic Half-Semiconductor (HSC) gaps in co-doped CdS: Ab-initio study

M. Boudjelal[a], A. Belfedal[a], B. Bouadjemi[b,*], T. Lantri[b], R. Bentata[b], M. Batouche[c], R. Khenata[c]

[a] Laboratoire de Chimie Physique des Macromolécules et Interfaces Biologique Département de Biologie, Université de Mascara, Algeria
[b] Laboratory of Technology and Solid's Properties, Faculty of Sciences and Technology, Abdelhamid-Ibn-Badis University, BP 227, Mostaganem 27000, Algeria
[c] Laboratoire de Physique Quantique de la Matière et de la Modélisation Mathématique (LPQ3M), Université de Mascara, 29000, Algeria

ARTICLE INFO

Keywords:
Half-Semiconductor (HSC)
Co doped CdS
DFT
Magnetism
Spintronic applications

ABSTRACT

In this work we have used the density functional theory (DFT) to study structural, magnetic and electronic properties of Co doped CdS in the zinc-blende (ZB) phase. Three approximations have been used to treat the exchange-correlation potential: the (PBE) GGA, (PBE) GGA + U and the model of Tran–Blaha modified Becke–Johnson potential (TB-mBJ). The on–site Coulomb interaction correction given by the Hubbard U has been calculated by the local density approximation constraint for the Co electronic orbitals. The theoretical results show that all the properties under study are affected by the doping of Co atom. Co doped CdS becomes a Ferromagnetic Half-Semiconductors (HSC). The total magnetic moment increases with increasing Co concentration; reaching the value of 9 (in the units of Bohr magneton) at high concentration (x = 18.75 %). The total magnetic moment value is an integer in the GGA + U and TB-mBJ approximations. Furthermore, to validate the effects resulting from the exchange splitting process, we have calculated the values of the spin-exchange constants $N_{0\alpha}$ and $N_{0\beta}$, respectively. All these changes make CdS:Co extremely interesting system for the spintronic applications.

1. Introduction

Recently, diluted magnetic semiconductors (DMSs) with room-temperature ferromagnetism have attracted considerable attentions for possible applications in spintronic and optoelectronic [1]. These approaches aim to exploit the spin of the electron and its charge to improve functionalities of micro-electronic properties. The diluted magnetic semiconductors (DMS) are also the subject of many studies in recent years because of their interesting electronic and magnetic properties [2]. Another important feature of the DMSs is that the energy band gap and other physical parameters can be controlled by varying the composition of magnetic ions in these materials [3].

CdS is one of these compounds, known for its wide band gap energy (2.42 eV), its hexagonal/cubic crystalline structure, comparatively low resistivity, high photoconductivity, large absorption coefficient and high refractive index (between 2.5 and 2.7) in the visible range [3,4]. These properties make CdS a promising material for applications such as in solar cells, optical detectors and other optoelectronic devices [5,6]. Currently, semi-magnetic semiconductors (SMSC) with Co^{+2} as a magnetic ion have been the focus of increasing interest due to the existence of the spin–orbit interaction and large exchange interaction. II–VI group compounds have

* Corresponding author.
E-mail address: bbouadjemi@yahoo.fr (B. Bouadjemi).

https://doi.org/10.1016/j.cjph.2019.09.004
Received 22 June 2019; Received in revised form 16 August 2019; Accepted 6 September 2019
Available online 12 September 2019

been mostly studied using Mn^{+2} and Co^{+2} ions [7]. This kind of doping significantly modifies the optical, electrical and magnetic properties due to the presence of p-d orbital hybridization and spin–spin coupling [8]. Doping could also change the crystal symmetry and structural morphology [9]. Many theoretical and experimental researches were performed to obtain semiconductors with improved ferromagnetic properties. Dietl et al. [10] suggested that 5% of Mn doping in the CdS material leads to an n-type semiconductor with a Curie temperature of 200 K. Sato and Katayama-Yoshida [11] studied the effects of the dopants (Fe, Co, Ni, V and Cr) in ZnX (X = Se, Te, O) and confirmed that the ferromagnetic state is more favorable in energy than the antiferromagnetic one. Recently, Xiao and Wang [12] have investigated non-magnetic dopants (B, C, N and O) in the CdS monolayer and confirmed the emergent ferromagnetism in these systems. The effect of Pd doping in CdS were studied by Ren et al. [13]. They found that the Pd-doped CdS was spin polarized at 100% and the hybrid chain mechanism Pd(4d)-S(3p)-Cd (4d)-S(3p)-Pd(4d) formed by p-d coupling is responsible for the long-range FM order. The Co-doped CdS nanowires have ferromagnetic behavior at room temperature. These nanowires have been synthesized by many researchers where they have observed ferromagnetism in Co-doped CdS synthesized by a high-energy electron irradiation [14,15]. However, Saravanan et al. synthesized CdS doped with Co nanoparticles by chemical Co precipitation [16]. The Co-doped CdS nanocrystals with controllable morphology (quantum dots and nano-rods) have also been reported by Zha et al. [17]. The results indicated that the Co-doping was favorable to the formation of nano-rod structures during a short reaction time. Recent theoretical researches have been conducted on a wide variety of high concentrations of DMSs doped with transition materials such as: $Cd_{1-x}Mn_xS$ [18], $Cd_{1-x}Cr_xS$ [19], $Cd_{1-x}Co_xS$ [20], $Cd_{1-x}Fe_xS$ [21], and $Cd_{1-x}Ni_xS$ [22]. All these studies predicted that Co is apt to induce Half Metallicity (HM) in suitable materials.

Structural forms of CdS exist in three configurations (Wurtzite, Zinc-blende, and rock-salt forms). It should be noted that majority of the previous reports were on the wurtzite (WZ) structure of CdS doped with Co. It should also be noted that no theoretical research has been reported on the study of the doping effect on CdS with low concentrations of Co in the zinc-blende phase on the magnetic and electronic properties. This motivates us to explore the effect of Co doping on the electronic and magnetic properties of CdS with Zn-blende structure. In addition, we have also chosen Co because it still stimulates the experimental studies [23] and allows us to compare the results of this study with the experimental and theoretical ones available in the literature.

In this study we have reported the structural, magnetic and electronic properties in the zinc-blende phase of $Cd_{1-x}Co_xS$ alloys at different x values (0, 0.0625, 0.125, and 0.1875). We have used CdS 1_2_2 super cell by employing the theory of the spin-polarized density function, in the framework of generalized gradient approximation (GGA), GGA + U and the Becke–Johnson model (TB-mBJ).

Our goal is to develop models for materials having at the same time semiconducting and ferromagnetic properties and to explore the role of the transition metal Co on the electronic, magnetic and electronics properties of the compound $Cd_{1-x}Co_xS$.

This paper has been organized as follows: in Section 2, the calculation details are described. Section 3 is comprised of the various results of the calculated properties. We also discuss the various aspects of these results in this section. Finally, Section 4 summarizes the conclusions of this study.

2. Calculation method

All the calculations reported in this work have been performed using the potential enhanced (full potential) linear wave plane (FP-LAPW) method implemented in the Wien2k code [24,25]. Three approximations have been used to express exchange-correlation potential: the generalized gradient approximation (GGA) [26], GGA + U [27] and TB-mBJ [28]. It should be mentioned that the GGA is well suited for solids in their ground state properties, but not well adapted for excited state properties. This is because the GGA contains self-interaction errors (SIE) and does not show discontinuity in derivative, which is important for band gap calculations. The Hubbard U term in GGA has been added to eliminate the self-interaction error (SIE) and to calculate the effective Coulomb on-site repulsion where correlations are expected to be processed correctly [29]. The DFT + U functions are good for the excited states; especially for the localized electronic states (typically the 3d and 4f electrons). The on-site Coulomb interaction U and that due to magnetic exchange energy J, can be expressed by a single effective parameter $U_{eff} = U - J$. We have computed U_{eff} using the constraint method developed by Anisimov et al. [30,31]. To use this method, a supercell of 32-atoms is built and the hybridization between 3d orbital of one atom (Co in the present work) and all the other orbitals is removed by placing the d-states in the core ones, U_{eff} values of $Cd_{1-x}Co_xS$ are then calculated using the following expression:

$$U_{eff} = \varepsilon_{3d\uparrow}\left(\frac{n+1}{2}, \frac{n}{2}\right) - \varepsilon_{3d\uparrow}\left(\frac{n+1}{2}, \frac{n}{2} - 1\right) - \varepsilon_F\left(\frac{n+1}{2}, \frac{n}{2}\right) + \varepsilon_F\left(\frac{n+1}{2}, \frac{n}{2} - 1\right) \quad (1)$$

$\varepsilon_{3d\uparrow}$ represents the rotation energies of 3d (spin-up) orbitals of the transition metal, ε_F represents the Fermi level and n is the electron number within the 3d orbitals. Another scheme was developed by Tran and Blaha; they modified the potential of Becke-Johnson to develop a semi-local TB-mBJ function. This is not a significant hybrid function and it can improve the band gap for a variety of semiconductors with electrons in the d or f orbitals [28].

CdS in a zinc-blende structure belongs to the F-43m space group (No. 216) and the experimental lattice constant is around 5.83 Å [32]. Its primitive unit cell has a CdS molecular unit where the Cd atom is located at (0, 0, 0) and the S atom at (0.25, 0.25, 0.25). We have simulated our compounds $Cd_{1-x}Co_xS$ for x = 0, 0.0625, 0.125 and 0.1875, in a super cell of 32 atoms created from (1_2_2) units, as illustrated in Fig. 1. The electronic configurations used to carry out theoretical computations of Cd, S and Co are respectively, $4d^{10}5s^2$, $3s^23p^4$ and $3d^74s^2$. Muffin-tin (MT) sphere radii have been selected as equal to 2.43 a.u. for both Cd and Co and 2.33 a.u. for S. Further, the $R_{MT}{*}K_{max}$ parameter have been chosen to be 8, with R_{MT} as the smallest muffin-tin radius and K_{max} as the maximum modulus of the reciprocal lattice vector k in the first Brillouin zone. The total number of K points was 100, and we have followed the Monkhorst–Pack scheme [33] to sample the Brillouin zone. The energy convergence criterion for self-consistency is less than

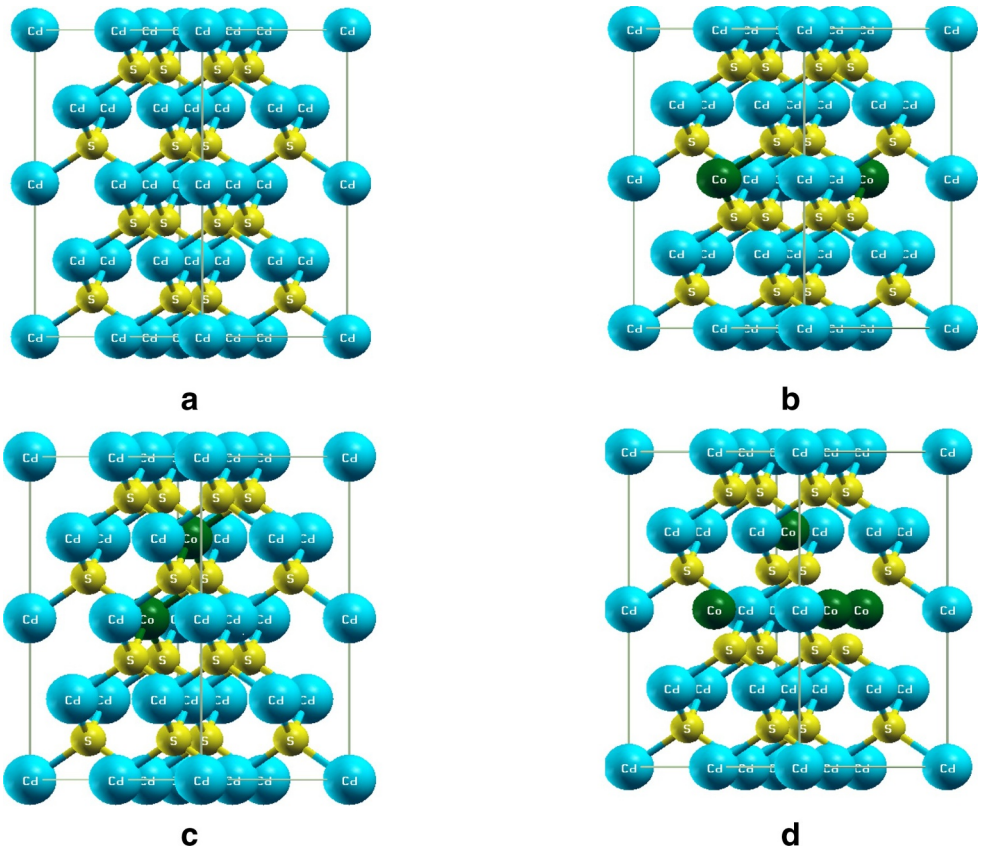

Fig. 1. The crystal structure of bulk $Cd_{1-x}Co_xS$ with **(a)** $x = 0$, **(b)** $x = 0.0625$, **(c)** $x = 0.125$, and **(d)** $x = 0.1875$ supercell of 32 atoms.

10^{-4} eV. The GGA approximation is applied to treat the structural properties whereas the electronic and magnetic properties of the compound under study have been examined by employing the (PBE-GGA + U) and TB-mBJ. The U_{eff} values for Co have been calculated and taken as 0.49 Ry (6.66 eV).

The stability of ferromagnetic state of these compounds has been verified by the total energy difference ($\Delta E_{FM} = E_{FM} - E_{AFM}$) of the supercells between the AFM and FM ground states; if this difference is positive, the FM state, having the lowest energy after structure optimization, is stable, as discussed in the next section.

3. Results and discussions

3.1. U_{eff} calculation

The Co atom has 7 electrons in the 3d orbital (t_2g^5, eg^2). We have forced the 3d electrons into the core to prevent all kinds of hybridizations with the other orbital and then performed two calculations for each atom. In the first step, we have calculated for the Co atom where 4 electrons are configured in up and the other 3.5 electrons in down (see Table 1, Calc. 1). In the second step, the calculation has been carried out by putting 4 electrons up and 2.5 electrons down (see Table 1, Calc. 2). We have obtained $\varepsilon_{3d\uparrow}$ energies by a weighted sum of energies $\varepsilon_{3d}{}^{5/2}$ and $\varepsilon_{3d}{}^{3/2}$. The obtained values for the energies (in Ry): $\varepsilon_{3d}{}^{5/2}$, $\varepsilon_{3d}{}^{3/2}$, $\varepsilon_{3d\uparrow}$ and ε_F have been summarized in Table 1.

Table 1
The different values of energies (in Ry): $\varepsilon_{3d}{}^{5/2}$, $\varepsilon_{3d}{}^{3/2}$, $\varepsilon_{3d\uparrow}$, ε_F and U_{eff}.

Compound	$\varepsilon_{3d}{}^{5/2}$		$\varepsilon_{3d}{}^{3/2}$		$\varepsilon_{3d\uparrow}(\frac{n+1}{2}, \frac{n}{2})$	$\varepsilon_{3d\uparrow}(\frac{n+1}{2}, \frac{n}{2}-1)$	$\varepsilon_F(\frac{n+1}{2}, \frac{n}{2})$	$\varepsilon_F(\frac{n+1}{2}, \frac{n}{2}1)$	U_{eff}
	Calc.1	Calc.2	Calc.1	Calc.2					
$Cd_{0.9375}Co_{0.0625}S$	0.025	0.038	−0.419	−0.404	0.038	−0.411	0.198	0.247	0.498
$Cd_{0.875}Co_{0.125}S$	0.037	0.050	−0.397	−0.382	0.043	−0.389	0.227	0.288	0.493
$Cd_{0.8125}Co_{0.1875}S$	0.039	0.053	−0.389	−0.374	0.046	−0.381	0.242	0.307	0.492

Table 2
The optimization of calculation, equilibrium lattice constant a_0, bulk modulus B and its pressure derivative B′ with $x = 0$, 0.0625, 0.125 and 0.1875 by using the PBE-GGA approximation. And total energy difference between AFM and FM configurations ΔE (eV) for $Cd_{1-x}Co_xS$ using the PBE-GGA + U.

Compound	Lattice parameter a_0 (A°)			Bulk modulus B (GPa)			B′			ΔE(eV)
	This work	Calc.	Exp.	This work	Calc.	Exp.	This work	Calc.	Exp.	Calc.
CdS	5.95	5.863[a] 5.97[b]	5.83[d]	53.02	65.7[a]	64.3[d]	4.39	4.494[a]	–	–
$C_{0.9375}Co_{0.0625}S$	5.91	5.809[c]		56.77	66.34[c]		4.12	4.49[c]	–	0.63
$Cd_{0.875}Co_{0.125}S$	5.88	–		57.49	–		4.14	–	–	0.031
$Cd_{0.8125}Co_{0.1875}S$	5.85	–		58.10	–		4.13	–	–	0.032

[a] Ref. [36]
[b] Ref. [37]
[c] Ref. [38]
[d] Ref. [39]

3.2. Structural properties and stability

Determination of structural properties is the first and fundamental step in any theoretical calculation of properties of materials. The equilibrium structural parameters have been obtained by computing the total energy versus volume at (T = 0 K) using the Birch–Murnaghan's equation of state [34,35].

$$E_{Tot}(V) = E_0(V) + \frac{B_0(V)}{B`(B` - 1)}\left[B\left(1 - \frac{V_0}{V}\right) + \left(\frac{V_0}{V}\right)^{B`}\right] \quad (2)$$

Where, E_0,B,$B^{\backslash}$,V_0 are the total internal energy, the bulk modulus, the pressure derivative of the bulk modulus and the volume of the elementary cell at equilibrium, respectively.

The Birch–Murnaghan's equation of state gives a good fit of the energy as a function of the volume of the primitive cell. The total energy as a function of the volume for the compounds $Cd_{1-x}Co_xS$ at x equals to 0, 0.0625, 0.125, and 0.1875, respectively with polarized spin, has been studied by employing the PBE-GGA parameterization. For each curve we notice that the energy has a minimum for a given mesh parameter. The obtained results from fitting of equilibrium structural parameters such as, the lattice constant (a_0), the bulk modulus (B_0), and its first pressure derivative ($B^{\backslash}$), have been summarized in Table 2. It is observed that the lattice constants of ternary $Cd_{1-x}Co_xS$ alloys decrease with augmenting x concentration of Co impurity. This may be ascribed to smaller atomic radii of Co^{2+} (0.74 Å) compared to that of Cd^{2+} (0.97 Å). The obtained results are in excellent agreement with other theoretical values [36–38] and experimental data [39] found in the literature.

To further investigate the relative stability of the ferromagnetic (FM) state with respect to the antiferromagnetic (AFM) ones, we have constructed super cells of 1_2_2 to get even numbers of Co element for switching spin up and down states and calculated the AFM and FM total energies for all Co concentrations with their optimized equilibrium lattice constants. Using the GGA + U method, the calculated total energy difference between the AFM and FM states ($\Delta E = E_{FM} - E_{AFM}$) of $Cd_{1-x}Co_xS$ has been summarized in Table 2. The FM order has lower total energy compared to AFM order, and consequently FM state has been predicted to be the stable configuration in these ternary alloys $Cd_{1-x}Co_xS$. Furthermore, we have calculated the formation energy of the Co doped CdS defined by Bai et al. [40,41] and Alay-E-Abbas [42]:

$$E_f = E_t(Cd_aCo_bS_c) - aE_{bulk}(Cd) - bE_{bulk}(Co) - cE_{bulk}(S) \quad (3)$$

Where, $E_tCd_aCo_bS_c$ is the total energy of the supercell with n Cd atoms replaced by Co atoms and E_{bulk}(Cd), E_{bulk}(Co) and E_{bulk}(S) are the total energies per atom of fully bulk Cd, Co, and S, respectively and a, b, c are the numbers of Cd, Co, and S atoms in the unit cell formation. The calculated formation energy E_f is predicted to be −1.41 eV, −1.36 eV, and −1.22 eV at $x = 0.0625$, 0.125 and 0.1875, respectively. The negative formation energy indicates that the Co-doped CdS can be synthesized experimentally. The order of the formation energy is $Cd_{0.9375}Co_{0.0625}S < Cd_{0.875}Co_{0.125}S < Cd_{0.8125}Co_{0.1875}S$.

3.3. Electronic properties

3.3.1. Band structure

The objective of computed band structure is mainly to predict band gap energy value, which usually is considered as an important parameter for the optoelectronics and spintronic device applications. This parameter is defined as the difference between the lowest energy conduction bands of majority (minority) spin and the absolute value of the highest energy valence bands of majority (minority) spin [43].

Structures of spin polarized electronic bands with up and down spin states have been calculated for the ferromagnetic $Cd_{1-x}Co_xS$ for different x values ($x = 0$, 0.0625, 0.125 and 0.1875). The band structures have been evaluated at their equilibrium lattice parameter using three different approaches: GGA, GGA + U and TB-mBJ schemes. These predictions are served to identify the precise

Table 3
Calculated total and local magnetic moments (μ_B) and in the interstitial sites for $Cd_{1-x}Co_xS$ with $x = 0$, 0.0625,0.125 and 0.1875 using the (a) PBE-GGA, (b) PBE-GGA + U and (c) Tb-mBJ approximations.

	Compound	M^{To}	m^{Co}	m^{Cd}	m^{S}	m^{inter}
BPE-GGA	$Cd_{0.9375}Co_{0.0625}S$	3.0026	2.0481	0.0102	0.0604	0.2001
	$Cd_{0.875}Co_{0.125}S$	5.9959	2.4823	0.0060	0.1204	0.4012
	$Cd_{0.8125}Co_{0.1875}S$	8.9851	2.4915	0.0037	0.2315	0.8287
PBE-GGA + U	$Cd_{0.9375}Co_{0.0625}S$	3.0013	2.7297	0.0018	0.0968	0.3652
	$Cd_{0.875}Co_{0.125}S$	5.9999	2.8409	0.0037	0.0194	0.1940
	$Cd_{0.8125}Co_{0.1875}S$	9.0001	2.8419	0.0034	0.0219	0.2951
Tb-mBJ	$Cd_{0.9375}Co_{0.0625}S$	3.0000	2.7362	0.0003	0.0328	0.1153
	$Cd_{0.875}Co_{0.125}S$	6.0000	2.7304	0.0003	0.0635	0.2340
	$Cd_{0.8125}Co_{0.1875}S$	9.0001	2.7297	0.0027	0.0663	0.3652

potential to be used in exploring spintronic and optoelectronics application possibilities. The values of the band gap (Eg) obtained for minority-spin and the majority spin gap are given in Table 3. It is noted that Eg obtained with TB-mBJ are higher and improved than those obtained with PBE-GGA and PBE-GGA + U. This is because the TB-mBJ semi local exchange correlation potential can provide perfect band gaps compared with the LDA and different versions of the GGA approximation for semiconductors and insulators [44]. The band gap values of pure CdS is about 1.008 eV by PBE-GGA and 2.52 eV by TB-mBJ method; the latter is very close to the experimental value [23,45]. This confirms the reliability of our calculations. We, therefore, have adopted the TB-mBJ formalism in all the subsequent calculations (see Fig. 2). The electronic band structures of $Cd_{1-x}Co_xS$ for $x = 0.0625$, 0.1250 and 0.1875 are shown in Fig. 4. One can see clearly that the band gap value for spin up channel is different from that in the spin down one for all three approaches compared to that of the pure CdS (Fig. 3(a) and (b), which is the same for both spin directions).

Different exchange-correlation schemes also yield different band gap values (see Table 4) that indicates that Co doped CdS becomes a Ferromagnetic Half-Semiconductor (HSC). We have found that band gap up values of $Cd_{1-x}Co_xS$ for $x = 0.0625$, 0.1250 and 0.1875 compounds using GGA + U are 1.07, 1.11, and 1.19 eV, respectively; these values for $x = 0.0$, 0.0625, 0.1250 and 0.1875 using the TB-mBJ are 2.523, 2.579, 2.611 and 2.572 eV, respectively. Under both the schemes the band gap increases with increasing Co doping. On the other hand, use of simple GGA for $x = 0$, 0.0625, 0.125 and 0.1875 results in gap up values equal to 1.008, 0.975 0.0.897, 0.679, respectively. Interestingly, within simple GGA the band gap decreases with increasing Co doping. It is noteworthy that the results obtained with TB-mBJ are improved compared to those obtained with PBE-GGA and PBE-GGA + U and correspond closely to available experimental data [23] (see Fig. 2). However, the Co doped CdS has preserved the nature of the direct forbidden band gap of pure CdS. Both the top of the valence band and the bottom of the conduction band is located at the Γ point of the Brillouin zone, exhibiting ferromagnetic semi-semiconductors character. Therefore, we can conclude that Co doping has changed the electronic nature of CdS from semiconductor to Ferromagnetic Half-Semiconductor materials (HSC), which are promising materials for use in spintronic applications [46].

3.3.2. Density of states

To get a deeper understanding of the electronic properties and to see the impact of Co doping on them, we have calculated the

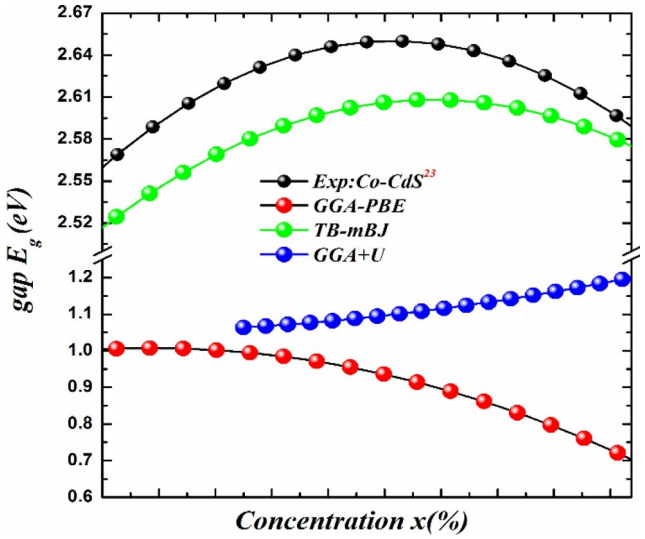

Fig. 2. Band gap values calculated with different approximations of $Cd_{1-x}Co_xS$ without $x = 0.0625$, 0.125, and 0.1875 in comparison with experimental results (all values are given in eV).

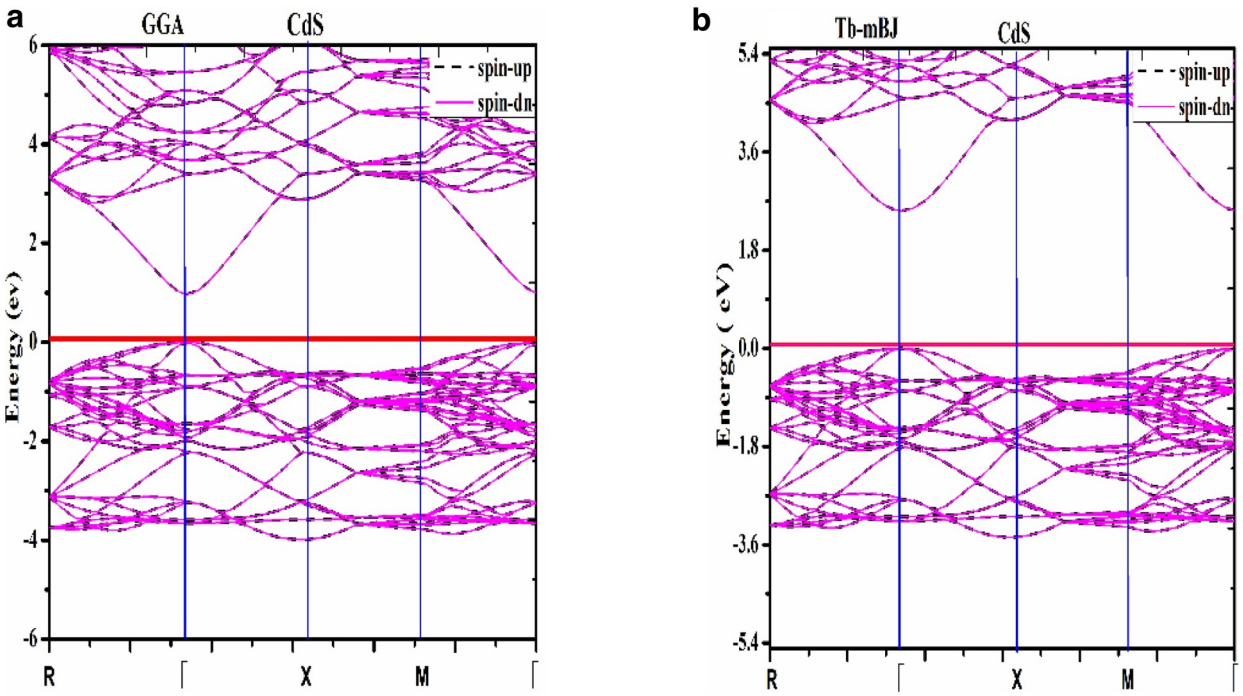

Fig. 3. Spin-polarized electronic band structures for pure CdS using PBE-GGA and TB-mBJ approximations.

total (TDOS) and partial (PDOS) density of states for the pure CdS and for $Cd_{1-x}Co_xS$ with $x = 0$, 0.0625, 0.125 and 0.1875, respectively, using the TB-mBJ in both spin (up and down) channels (see Fig. 5).

Fig. 5(a) illustrates that CdS is a non-magnetic semiconductor. The valence band (VB) is mainly due to states 3p of S with a small admixture of states 5s of Cd, while the conduction band (CB) is dominated by states 5s of Cd with a small number of states 3p of S. During the formation of CdS, Cd provides 2 electrons to S and the ionic states of Cd^{2+} and S^{2-} are formed. On the other hand, the electrons of S-3p and Cd-5s are shared, covalent bond is formed, and therefore, the compound CdS show significant covalent character. When Co ($3d^74s^2$) is doped in CdS, two of its electrons establish bonds with two neighboring S atoms, while the rest of the electrons of the orbital d are exposed to the effect of the tetrahedral crystalline field. The tetrahedral crystal field formed by the surrounding S ions splits the five-fold degenerate 3d states of Co into a two-fold degenerate eg ($d_{(x2)-(y2)}$ $d_{(z2)}$), and a three -fold degenerate t_2g (d_{xy},d_{yz}, d_{xz}), states [47]. This separation in energy is due to the strong p-d exchange interaction between the 3d states of Co atoms and the 3p orbital of S. The spin-polarized total (TDOS) and partial (PDOS) density of states of $Cd_{1-x}Co_xS$ with $x = 0$, 0.0625, 0.125 and 0.1875 are shown in Fig. 5(b)–(d). These plots show that the valence bands of the two spin directions are dominated by the major contribution of p (S) and 3d (Co) states and minor contribution of s (S) and d (Cd) states are fully occupied and located between ~ -4.1 and -0.1 eV in the energy ranges of $\sim -3.8-0.2$ eV for $Cd_{0.9375}Co_{0.0625}S$, $\sim -3.9-0.2$ eV for $Cd_{0.875}Co_{0.125}S$, and $\sim -4.0-0.2$ eV for $Cd_{0.8125}Co_{0.1875}S$, and the unoccupied 3d (t_2g) states of minority spin are located at the bottom of the conduction band, around 2.6 eV, 2.7 eV for $x = 0.0625$, 0.125, respectively and located between ~ -2.2 eV and 3.0 eV for $x = 0.1875$. Moreover, Fig. 5(b)–(d) reveal that, as a result of the doping, a spin asymmetric shape of TDOS arises which means the presence of magnetism and additional peaks in the PDOS. In the VB, these peaks originate from the 3d (t_2g, eg) electronic states of Co and in the CB they are mainly from the Co-3d (t_2g) electronic states. In fact, the latter ones form the minimum of the CB in spin down direction leading to a band gap value different from that of spin up configuration. No d-state peak of Co lies at E_F, which confirms the semiconducting behavior of $Cd_{1-x}Co_xS$ with the addition of magnetic dopant. This result also confirms the Ferromagnetic Half-Semiconductor (HSC) character of our compounds $Cd_{1-x}Co_xS$ as found from the band structures. By increasing Co doping concentration, the degree of hybridization between Co-3d (t_2g) and S-3p electronic orbitals increases significantly.

3.3.3. Magnetic properties and exchange constants

In order to elucidate the important role of the conduction band and the valence band on the exchange splitting, as observed in the electronic band structure of $Cd_{1-x}Co_xS$ compounds, the s–d exchange $N_{0\alpha}$ and the p–d exchange $N_0\beta$ have been calculated based on the exchange field field theory. These two constants characterize the exchange splitting and are computed using the expression for spin Hamiltonian given by

$$H = -N_0\beta s.\ S \tag{4}$$

where N_0 and β are the cations content and p-d exchange energy, respectively, whereas s and S represent, respectively, free hole and the Co impurity spins. The exchange constants can be directly calculated from the band structure and the magnetic properties by

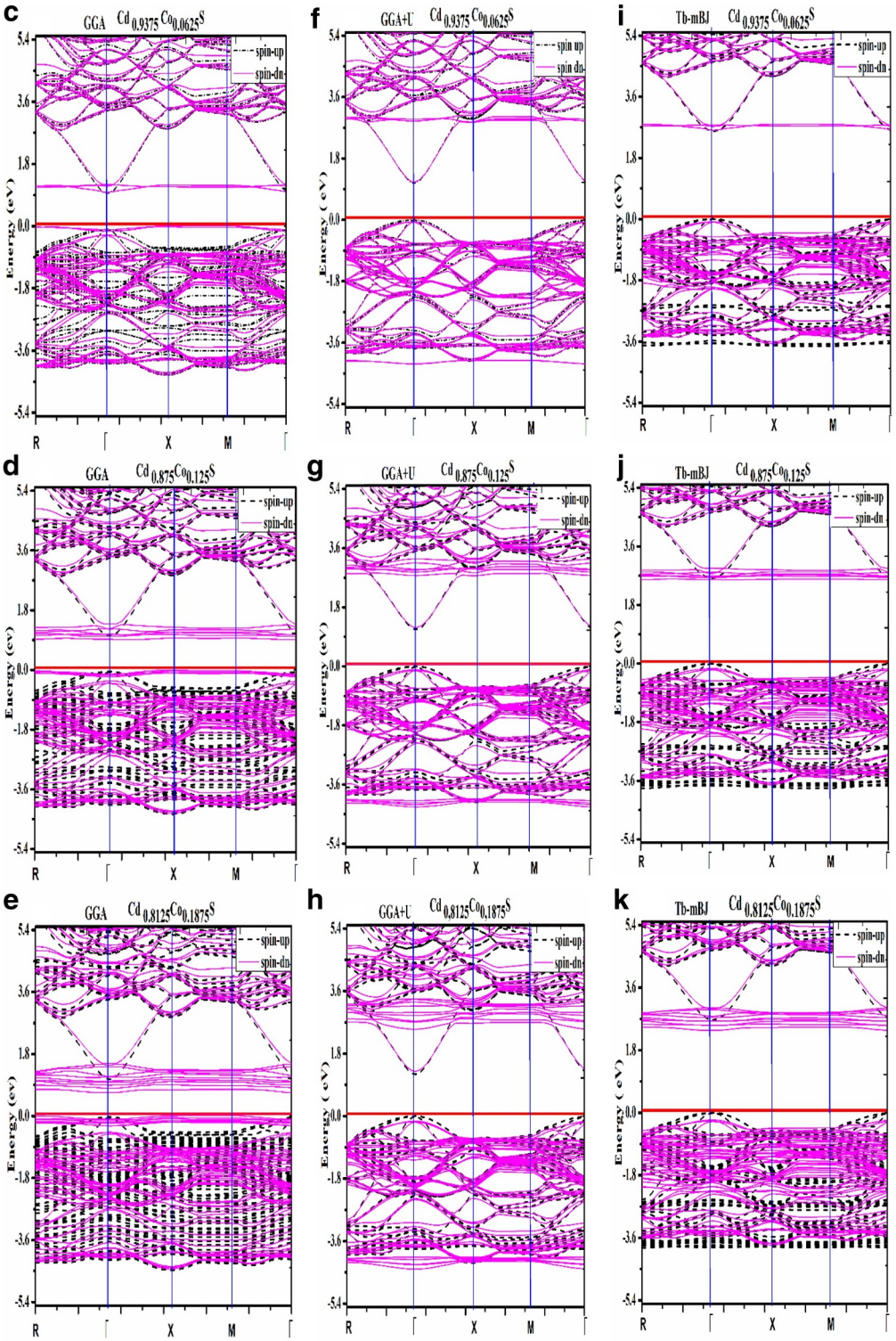

Fig. 4. Spin-polarized electronic band structures for $Cd_{1-x}Co_xS$ with $x = 0.0625$, 0.125 and 0.1875 using PBE-GGA, PBE-GGA + U and TB-mBJ approximations.

Table 4
Band gap energy $Eg^{\Gamma-\Gamma}$ of $Cd_{1-x}Co_xS$ at $x = 0.00$; 0.0625; 0.125 and 0.1875 using the BPE-GGA, PBE-GGA + U and TB-mBJ approximations.

	GGA (eV)		*GGA + U (eV)*		*TB-m BJ (eV)*		$Eg^{\Gamma-\Gamma\ (Exp)}$
	up	dn	up	dn	up	Dn	
CdS	1.008	1.008	-	-	2.523	2.523	2.56[a], 2.42[b]
$Cd_{0.9375}Co_{0.0625}S$	1.042	0.975	1.071	1.158	2.579	2.697	
$Cd_{0.875}Co_{0.125}S$	1.056	0.897	1.115	1.273	2.617	2.695	2.65[a] (a: x = 0.1)
$Cd_{0.8125}Co_{0.1875}S$	1.084	0.679	1.198	1.426	2.667	2.572	2.57[a] (a: x = 0.2)

[a] Ref. [23].
[b] Ref. [48].

supposing the usual kondo interaction, which are known as [48]

$$N_{0\alpha} = \frac{\Delta E_c}{x\langle S\rangle}, \tag{5}$$

$$N_{0\beta} = \frac{\Delta E_v}{x\langle S\rangle} \tag{6}$$

where $\Delta E_v = (E_v^{\downarrow} - E_v^{\uparrow})$ is the valence band edge splitting and $\Delta E_c = (E_c^{\downarrow} - E_c^{\uparrow})$ is the conduction band edge splitting, x is the Co concentration and $\langle S\rangle$ is the half of the computed magnetization per Co ion.

The calculated values of $N_{0\alpha}$, $N_{0\beta}$, ΔE_v, ΔE_c using the TB-mBJ are displayed in Table 5. It can be seen that the exchange constant $N_{0\alpha}$ decreases, whereas those of $N_{0\beta}$ increases with increasing Co concentration of x from 0.0625 to 0.1875, confirming the magnetic character of these alloys. The negative sign of both $N_{0\beta}$ and $N_{0\alpha}$ means that the double exchange mechanism exists in these compounds because the s-d and p-d interactions are parallel and give an FM character. Except for that of $N_{0\alpha}$ found in $Cd_{0.0625}Co_{0.9375}S$, we see that the conduction and the valence states are behaving in a same manner during the exchange splitting process.

The values of $N_{0\alpha}$ in all the compounds are more negative than $N_{0\beta}$ meaning that the exchange energy involves through the spin-down channel a ferromagnetic half semiconductor behavior in our systems.

The total and local magnetic moments calculated in the muffin-tin spheres and in the interstitial sites, for the compounds $Cd_{1-x}Co_xS$ with $x = 0.0625$, 0.125 and 0.1875, using GGA, GGA + U and TB-mBJ approximations, are summarized in Table 3. The magnetic moment of the Co obtained by GGA + U and TB-mBJ is around 2.84 μ_B and 2.73 μ_B, respectively. These values are quite close to the value of 3μ_B for the Co^{2+} ion and larger than that obtained via GGA (2.48 μ_B). We have noticed that these higher values are comparable to other theoretical results [38]. On the other hand, the p-d hybridization between the Co-3d and the S-3p reduces the local magnetic moment on Co from its free state value and produces small local magnetic moments at the non-magnetic Cd and S host sites. This conclusion is consistent with the study carried out by Ladizhansky et al. [49]. Increasing the Co doping leads to an increase of the total magnetic moment which reaches the value of 9 μ_B per supercell at the highest x concentration ($x = 18.75$ %) considered in this study, in all the different approaches. These results confirm the ferromagnetic magnetic ground state of $Cd_{1-x}Co_xS$.

4. Conclusions

In this work, we have studied the structural, electronic, and magnetic properties of pure CdS and Co-doped CdS using the density functional theory (DFT) as implemented in the Wien2k code. Three different approaches have been adopted, namely, (PBE) GGA, (PBE) GGA + U and TB-mBJ. The Co doping of CdS at different concentrations changes its electronic ground state from a non-magnetic direct band gap semiconductor to Ferromagnetic Half-Semiconductor (HSC), preserving the direct band gap nature. The total magnetic moment obtained for $Cd_{1-x}Co_xS$ at $x = 0.0625$, 0.125 and 0.1875 generally comes from the d (t_{2g}) states of Co atoms of substitution with a weak contribution of the Cd and S ones. By increasing the Co dopant concentrations, the total magnetic moment increases and the Co-3d (t_{2g}) states strongly hybridize with the S-3p states. Furthermore, the negative sign of the exchange splitting operation of $N_{0\alpha}$ and $N_{0\beta}$ confirms the double-exchange mechanism caused by the s-d and p-d interaction in all the alloys under consideration. The theoretical results obtained by employing the TB-mBJ formalism are in good agreement with those deduced from the experimental and theoretical data. In this study, we have theoretically confirmed the semi-semiconducting nature of $Cd_{1-x}Co_xS$ with ferromagnetic spin ordering. Such compounds have potential to be used in the spintronic device applications.

CRediT authorship contribution statement

M. Boudjelal: Conceptualization, Formal analysis, Data curation, Writing - original draft, Writing - review & editing. **A. Belfedal:** Conceptualization, Formal analysis, Data curation, Writing - original draft, Writing - review & editing. **B. Bouadjemi:** Conceptualization, Formal analysis, Data curation, Writing - original draft, Writing - review & editing. **T. Lantri:** Conceptualization, Formal analysis, Data curation, Writing - original draft, Writing - review & editing. **R. Bentata:** Conceptualization, Formal analysis, Data curation, Writing - original draft, Writing - review & editing. **M. Batouche:** Conceptualization, Formal analysis, Data curation, Writing - original draft, Writing - review & editing. **R. Khenata:** Conceptualization, Formal analysis, Data curation, Writing - original draft, Writing - review & editing.

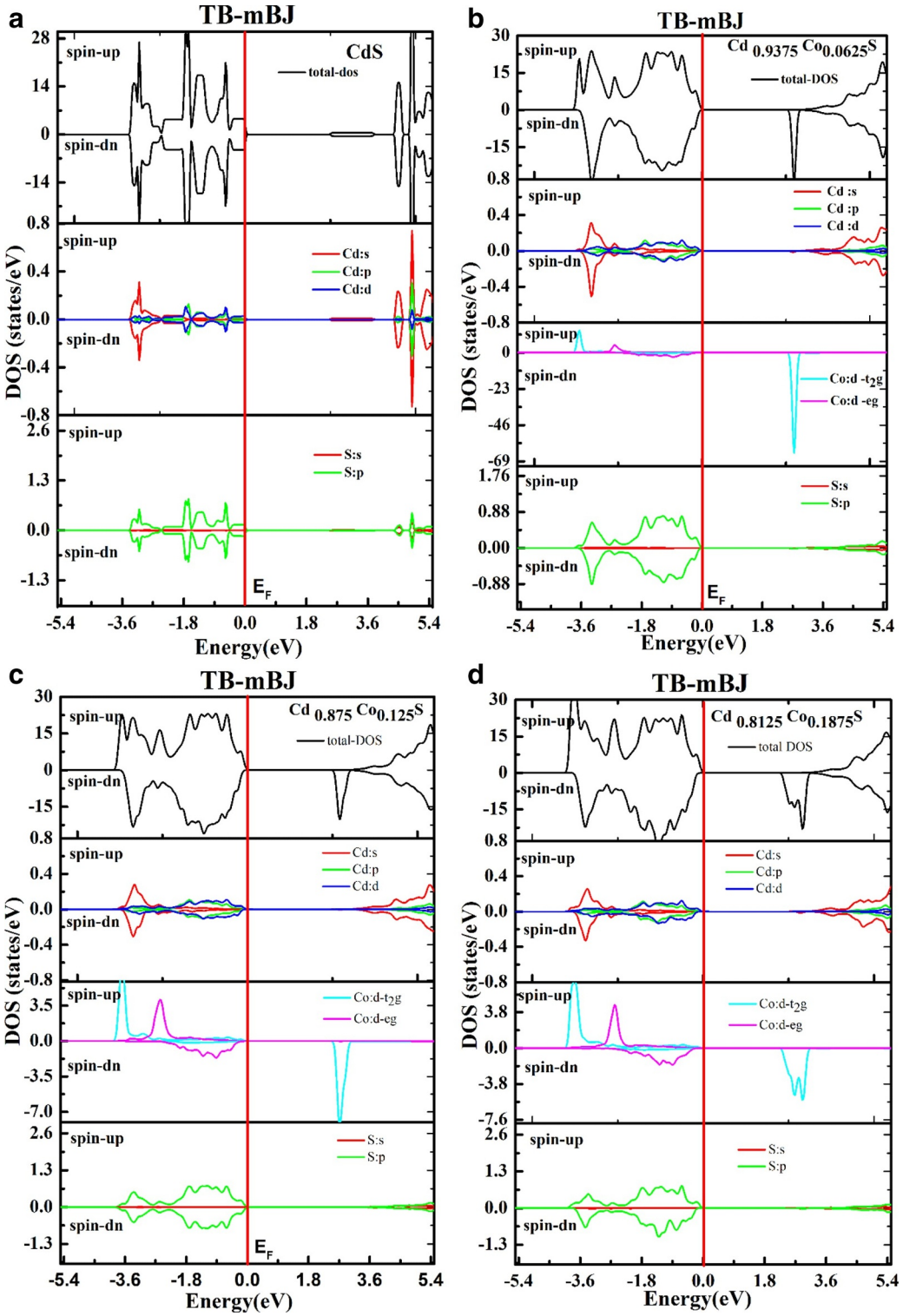

Fig. 5. Calculation of spin-dependent total and partial density of states for $Cd_{1-x}Co_xS$ using $x = 0$, 0.0625, 0.125 and 0.1875 using the TB-mBJ approximation.

Table 5
Calculated results of conduction band edge splitting (ΔE_c), valance band edge splitting (ΔE_v), exchange constants ($N_{0\alpha}$) and ($N_{0\beta}$) of each site in $Cd_{1-x}Co_xS$ alloys obtained using the TB-mBJ approximations.

Compound	ΔE_c	ΔE_v	$N_{0\alpha}$	$N_{0\beta}$
$Cd_{0.9375}Co_{0.0625}S$	0.0341	−0.0849	0.3639	−0.9058
$Cd_{0.875}Co_{0.125}S$	−0.0423	−0.1469	−0.2258	−0.7728
$Cd_{0.8125}Co_{0.1875}S$	−0.2982	−0.2085	−1.0603	−0.7413

Declaration of Competing Interest

None.

References

[1] A.I. Schindler, J.K. Furdyna, T.M. Giebultowicz, Diluted Magnetic Semiconductors, in: M. Jain (Ed.), World Scientific Publishing Co. Pvt. Ltd, Singapore, 1991, pp. 410–460.
[2] T.T. Xuan, J.Q. Liu, R.J. Xie, H.L. Li, Z. Sun, Microwave-assisted synthesis of CdS/ZnS:Cu quantum dots for white light-emitting diodes with high color rendition, Chem. Mater. 27 (2015) 1187–1193.
[3] Y. Dwarakanadha Reddy, B.K. Reddy, D. Sreekantha Reddy, D.R. Reddy, Optical and electrical studies of vapour phase grown Cd1−xCoxTe crystals, J. Spectrochim. Acta Part A 70 (2008) 934–938.
[4] M.A. Kamran, R. Liu, L.J. Shi, B. Zou, Near infrared emission band and origin in Ni(II)-doped CdS nanoribbons by CVD technique, J. Phys. Chem. C 117 (2013) 17777–17785.
[5] R. Tenne, V.M. Nabutovsky, E. Lifshitz, A.F. Francis, Unusual photoluminescence of porous CdS (CdSe) crystals, Solid State Commun. 82 (1992) 651–654.
[6] B. Su, K.L. Choy, Electrostatic assisted aerosol jet deposition of CdS, CdSe and ZnS thin films, Thin solid Films 361-362 (2000) 102–106.
[7] D.U. Bartholomew, E.K. Shu, A.K. Ramadas, S. Roodriguez, Electronic Raman scattering in $Cd_{1-x}Co_xSe$, Phys. Rev. B 39 (1989) 5865–5871.
[8] E.A. Kozlova, D.V. Markovskaya, S.V. Cherepanova, A.A. Saraev, E.Yu. Gerasimov, T.V. Perevalov, Novel photocatalysts based on Cd1_xZnxS/Zn(OH)2 for the hydrogen evolution from water solutions of ethanol, Int. J. Hydrogen Energy 39 (2014) 18758–18769.
[9] X. Duan, Y. Huang, R. Agarwal, C.M. Lieber, Single-nanowire electrically driven lasers, Nature 421 (2003) 241–245.
[10] T. Dietl, H. Ohno, F. Matsukura, Hole-mediated ferromagnetism in tetrahedrally coordinated semiconductors, Phys. Rev. B 63 (2001) 195205–195226.
[11] K. Sato, H. Katayama-Yoshida, First principles materials design for semiconductor spintronics, Semicond. Sci. Technol. 17 (2002) 367–376.
[12] W. Xiao, L.L. Wang, Magnetic properties in CdS monolayer doped with first-row elements: A density functional theory investigation, Phys. Status Solidi B 251 (2014) 1257–1264.
[13] M. Ren, C. Zhang, P. Li, Z. Song, X. Liu, The origin of ferromagnetism in Pd-doped CdS, J. Magn. Magn. Mater. 324 (2012) 2039–2042.
[14] D.S. Kim, Y.J. Cho, J. Park, J. Yoon, Y. Jo, M.H. Jung, (Mn, Zn) Co-Doped CdS Nanowires, J. Phys. Chem. C 111 (2007) 10861–10868.
[15] K. Bogle, S. Ghosh, S. Dhole, V. Bhoraskar, L.-F. Fu, M.-F. Chi, N. Browning, D. Kundaliya, G. Das, S. Ogale, Co:CdS diluted magnetic semiconductor nanoparticles: radiation synthesis, dopant-defect complex formation and unexpected magnetism, Chem. Mater. 20 (2008) 440–446.
[16] L. Saravanan, A. Pandurangan, R. Jayavel, Synthesis of cobalt-doped cadmium sulphide nanocrystals and their optical and magnetic properties, J. Nanopart. Res. 13 (2011) 1621–1628.
[17] J. Zhao, X. Li, Z. Li, Synthesis of Co-doped CdS nanocrystals by direct thermolysis of cadmium and cobalt thiolate clusters, J. Nanomater. 2015 (2015) 109734–109745.
[18] S. Nazir, N. Ikram, M. Tanveer, A. Shaukat, Y. Saeed, A.H. Reshak, Spin-polarized structural, electronic, and magnetic properties of diluted magnetic semiconductors Cd1-xMnxS and Cd1-xMnxSe in zinc blende phase, J. Phys. Chem. A 113 (2009) 6022–6027.
[19] S. Nazir, N. Ikram, S.A. Siddiqi, Y. Saeed, A. Shaukat, A.H. Reshak, First principles density functional calculations of half-metallic ferromagnetism in Zn1-xCrxS and Cd1-xCrxS, Curr. Opin. Solid State Mater. Sci. 14 (2010) 1–6.
[20] Y. Saeed, S. Nazir, A. Shaukat, A.H. Reshak, Ab-initio calculations of Co-based diluted magnetic semiconductors $Cd_{1-x}Co_xX$ (X = S, Se, Te), J. Magn. Magn. Mater. 322 (2010) 3214–3222.
[21] Ch. Bourouis, A. Meddour, First-principles study of structural, electronic and magnetic properties in Cd1xFexS diluted magnetic semiconductors, J. Magn. Magn. Mater. 324 (2012) 1040–1045.
[22] W. Benstaali, S. Bentata, H.A. Bentounes, A. Abbad, B. Bouadjemi, Influence of Ni–Ni separation on the optoelectronic and magnetic properties of Ni-doped cubic cadmium sulphide, J. Mater. Sci. Semicond. Process. 17 (2014) 53–58.
[23] R. Sathyamoorthy, P. Sudhagar, A. Balerna, C. Balasubramanian, S. Bellucci, A.I. Popov, K. Asokan, Surfactant-assisted synthesis of Cd1−xCoxS nanocluster alloys and their structural, optical and magnetic properties, J. Alloys Compd. 493 (2010) 240–245.
[24] K.M. Wong, M. Irfan, A. Mahmood, G. Murtaza, First principles study of the structural and optoelectronic properties of the A2InSbO6 (A = Ca, Sr, Ba) compounds, Optik 130 (2017) 517–524.
[25] P. Blaha, K. Schwarz, G.K.H. Madsen, D. Kvasnicka, J. Luitz, WIEN2k, An Augmented Plane Wave Plus Local Orbitals Program for Calculating Crystal Properties, 2th Edition, Vienna University of Technology, Vienna, 2001.
[26] J.P. Perdew, K. Burke, M. Ernzerhof, Generalized gradient approximation made simple, Phys. Rev. Lett. 77 (1996) 3865–3868.
[27] D.P. Rai, R.K. Thapa, An abinitio study of the half-metallic properties of Co2TGe (T = Sc, Ti, V, Cr, Mn, Fe): LSDA + U method, J. Korean Phys. Soc. 62 (2013) 1652–1660.
[28] F. Tran, P. Blaha, Accurate band gaps of semiconductors and insulators with a semi local exchange-correlation potential, Phys. Rev. Lett. 102 (2009) 226401–226405.
[29] V.I. Anisimov, J. Zaanen, O.K. Andersen, Band theory and Mott insulators: Hubard U instead of I, Phys. Rev. B 44 (1991) 943–954.
[30] V.I. Anisimov, O. Gunnarsson, Density-functional calculation of effective Coulomb interactions in metals, Phys. Rev. B 43 (1991) 7570–7574.
[31] V.I. Anisimov, I.V. Solovyev, M.A. Korotin, M.T. Czyżyk, G.A. Sawatzky, Density-functional theory and NiO photoemission spectra, Phys. Rev. B 48 (1993) 16929–19934.
[32] O. Madelung, M. Landolt–Borstein, Numerical Data and Functional Relationships in Science and Technology 17 b Springer, Berlin, 1982.
[33] J. Monkhorst, D. Pack, Special points for Brillouin –zone integration, Phys. Rev. B 13 (1976) 5188–5192.
[34] F.D. Murnaghan, The compressibility of media under extreme pressures, Proc. Natl. Acad. Sci. U.S.A. 30 (1944) 244–247.
[35] S.L. Shang, Y. Wang, D. Kim, Z.K. Liu, First-principles thermodynamics from phonon and Debye model: Application to Ni and Ni_3Al, Comput. Mater. Sci. 47 (2010) 1040–1048.
[36] Ch. Bourouis, A. Meddour, First-principles study of structural, electronic and magnetic properties in $Cd_{1-x}Fe_xS$ diluted magnetic semiconductors, J. Magn. Magn. Mater. 324 (2012) 1040–1045.
[37] Y.-X. Han, C.-L. Yang, Y.-T. Sun, M.-S. Wang, X.-G. Ma, The novel optical properties of CdS caused by concentration of impurity Co, J. Alloys Compd. 585 (2014)

503–509.
[38] H. Yahi, A. Meddour, Structural, electronic and magnetic properties of Cd1 – xTMxS (TM = Co and V) by ab-initio Calculation, J. Magn. Magn. Mater. 401 (2016) 116–123.
[39] O. Madelung, Landolt Borenstein, Numerical Data and Functional Relation-ships in Science and Technology 7b Springer, Berlin, 1982.
[40] J. Bai, J.M. Raulot, Y.D. Zhang, C. Esling, Xuzhou, L. Zuo, Crystallographic, magnetic, and electronic structures of ferromagnetic shape memory alloys $Ni_{2X}Ga$ X = Mn,Fe,Co from first-principles calculations, J. Appl. Phys. 109 (2011) 14908–14913.
[41] J. Bai, J.M. Raulot, Y.D. Zhang, C. Esling, X. Zhao, L. Zuo, Defect formation energy and magnetic structure of shape memory alloys Ni–X– Ga (X = Mn, Fe, Co) by first principle calculation, J. Appl. Phys. 108 (2010) 064904–064910.
[42] S.M. Alay-E-Abbas, K.M. Wong, N.A. Noor, A. Shaukat, Y. Lei, An ab-initio study of the structural, electronic and magnetic properties of half-metallic ferromagnetism in Cr-doped BeSe and BeTe, Solid State Sci. 14 (2012) 1525–1535.
[43] K.L. Yao, G.Y. Gao, Z.L. Liu, L. Zhu, Half-metallic ferromagnetism of zinc-blende CrS and CrP: a first-principles pseudopotential study, Solid State Commun. 133 (2005) 301–304.
[44] F. Tran, P. Blaha, Accurate band gaps of semiconductors and insulators with a semi-local exchange-correlation potential, Phys. Rev. Lett. 102 (2009) 226401–226405.
[45] C.X. Li, S.H. Dang, Doped with Ag and Zn effects on electronic structure and optical properties of CdS, Acta Phys. Sin. 61 (2012) 017202–017209.
[46] H. Moulkhalwa, Y. Zaoui, K. Obodo, A. Belkadi, L. Beldi, B. Bouhafs, Half-metallic and half-semiconductor Gaps in Cr-based chalcogenides: DFT + U calculations, J. Supercond. Novel Magn. 10 (2018) 1–15.
[47] X.Y. Cui, B. Delly, A.J. Freeman, C. Stamp fl, Magnetic metastability in tetrahedrally bonded magnetic III-Nitride semiconductors, Phys. Rev. Lett. 97 (2006) 016402–016406.
[48] S. Sanvito, P. Ordejon, N.A. Hill, First-principles study of the origin and nature of ferromagnetism in $Ga_{1-x}Mn_xAs$, Phys. Rev. B 63 (2001) 165206–165219.
[49] V. Ladizhansky, V. Lyahovitskaya, S. Vega, ^{113}Cd NMR study of transferred hyperfine interactions in the dilute magnetic semiconductors $Cd_{1-x}Co_xS$ and $Cd_{1-x}Fe_xS$ and impurity distribution in $Cd_{0.994}Co_{0-006}S$, Phys. Rev. B 60 (1999) 8097–8104.